



Dye-Sensitized Solar Cell Using Dyes Extracted from Roots of Lawsonia Inermis Plant

Abebaw Matebu^{1,2}, Siraye Esubalew^{1,2}, and Getachew Adam Workneh^{1,2*}

¹Department of Industrial Chemistry, Addis Ababa Science and Technology University, P.O. Box 16417, Addis Ababa, Ethiopia

²Sustainable Energy Centre of Excellence, Addis Ababa Science and Technology University, P.O. Box 16417, Addis Ababa, Ethiopia

Article Information

Article history:

Received 25 October 2025

Received in revised form 19 November 2025

Accepted 25 November 2025

Keywords:

Renewable energy
Dye sensitized solar cells
Natural dyes
Photoelectrochemical power
conversion efficiency

Corresponding author.

E-mail: getachew.adam@aastu.edu.et

(Getachew A)

<https://doi.org/10.69660/jmpt.v2i1.116>

Abstract

Dye-sensitized solar cells (DSSCs) from inorganic dyes such as Ru-containing compounds have the highest efficiency. However, noble metals are limited in amount, and costly in production. On the other hand, natural dyes have been a popular subject of research due to their cost efficiency, non-toxicity, and complete biodegradation. In this study, DSSC were fabricated utilizing natural dyes derived from the roots of the Lawsonia inermis (Henna) plant using different extraction solvents. Four selective extracts were obtained using solvents such as DMSO, isopropanol, acetone, and ethanol. The phytochemical analysis of the extracted crude products show that they contain pigments such as flavonoids, tannins, carotenes, and betalains. The effects of different extracting solvents are also explored by optical characteristics using an ultraviolet-visible spectroscopy which indicated carotenes as a major pigment in the extracts. The current-voltage (I-V) measurements to evaluate the fill factor and power conversion efficiencies showed that the dye sensitized solar cell based on DMSO solvent extracted dye has the highest efficiency of 0.15%, with a short circuit current density (J_{sc}) of 0.734 mA/cm², fill factor of 51.35% and open circuit voltage (V_{oc}) of 0.39V at one sun (100mW/cm²) illumination.

1. Introduction

As the world population grows, so do the associated energy demands, as well as worries about greenhouse gas emissions and climate change. These have sparked a worldwide hunt for alternate and environmentally friendly energy generation technologies. Solar energy, among the different renewable energy sources, provides abundant, quiet, and environmentally friendly electricity with significant potential for addressing global energy demands. Photovoltaics (PV) offers a cost-effective way to transform this plentiful and environmentally friendly energy source into electrical energy [1, 2].

Photovoltaic or solar (PV) cells are classified into generations as the first generation, second generation, and third generation solar cells [1]. The first generation's base structure is crystalline silicon, which can be single-crystal or multi-crystal. Amorphous silicon, cadmium telluride (CdTe), cadmium sulfide (CdS), and other thin-film solar cells make up the second generation. The last category includes non-silicon technologies such as the photoelectrochemical dye-sensitized solar cells (DSSCs), organic solar cells, quantum dot (QD) solar cells and perovskite solar cells [2].

The worldwide PV market has been dominated by crystalline silicon (Si)-based PV systems for the past five decades. This is primarily due to their advantageous characteristics, which include efficient energy production in direct sunlight, high photovoltaic performance stability in

all climatic situations, and maturity in their research and development operations and related material value chain. Nonetheless, Si-based PV systems have a number of disadvantages, including energy-intensive manufacturing processes, poor aesthetics, and poor photovoltaic efficiency at low light intensities. Their broad usage in building integrated photovoltaics (BIPV), portable electronics, and interior applications has been limited as a result of these factors [3–5].

In comparison to first generation solar cells, thin-film technology allows solar cells to employ substantially fewer materials necessary in a solar cell, significantly lowering production costs. Thin-film solar cells, on the other hand, have lower efficiency than first-generation solar cells, ranging between 10 and 20%. Furthermore, the unavailability and toxicity of the materials utilized have been the main limitations for thin-film solar cells in terms of large-scale manufacturing.

Dye sensitized solar cells (DSSCs), a third generation solar cell, are more cost-effective, have a simpler design, perform better in low light conditions, and are more environmentally friendly than silicon and other solar cells. As a result, DSSC is a promising solar energy harvesting technology with the potential to satisfy world energy consumption while having the least environmental impact [6].

A DSSC is made up of the following components: a working electrode made of nanocrystalline porous semiconductor, a sensitizer, a counter electrode, and an electrolyte. Since the first cell was discovered in 1991

by O'Regan and Grätzel, countless research and technology efforts have concentrated on enhancing its components so that better efficiency similar to regular silicon-based solar cells may be reached [7].

The electrolyte is a vital component of the DSSC that provides internal electrolytic conductivity, as it functions as an electron-transfer mediator with the role of regenerating the dye from an oxidised state, and is a key factor in determining the cells' performance [8]. As a result, different endeavours to research distinct forms of electrolytes have been made. Ionic conductivity is quite high in liquid electrolytes due to their high penetration power into semiconductor nanoporous film, slow recombination loss, and the fast regeneration of dye molecules [9].

The photosensitizer, which can convert solar energy into electricity with great efficiency, is the second most critical component of DSSCs. Various synthetic dyes based on novel metals such as ruthenium and osmium have been utilised in DSSCs, and these dyes have been shown to have the best potential to be used as sensitizers for DSSCs because they couple broad and intense charge transfer bands to favourable ground and excited state energies for electron injection reactions from the excited dye to TiO₂. However, substantial limitations such as scarcity, high cost, and laborious production limit their application in DSSCs [10]. As a result, we're concentrating our efforts on natural dyes, which provide benefits such as high molar extinction coefficients, ease of preparation, cheap cost, nontoxicity, environmental friendliness, and complete biodegradability. Natural pigments such as chlorophyll, carotene, and anthocyanin can be found in abundance in plant leaves, flowers, roots and fruits and they meet these criteria [11]. The visible light absorption property of these pigments, which makes them the best candidates for DSSCs fabrication, is shown in Figure 1.

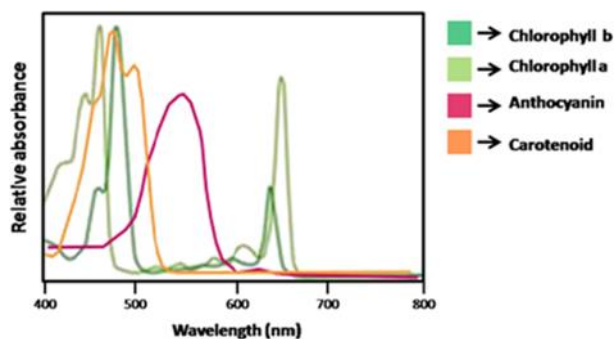


Figure 1. The absorption spectrum of chlorophyll a, chlorophyll b, anthocyanin and carotenoids in the range of visible light [22]

The Henna (*Lawsonia inermis*) plant's root, a traditional hair and skin colouring pigment is used as a natural dye sensitizer in the current investigation along with TiO₂ as a wide bandgap semiconductor, iodine-based electrolyte, and graphite-based counter electrode. As far as our knowledge dyes derived from *Lawsonia inermis* roots have not been reported as DSSC sensitizers and were optically evaluated by UV-Vis and FTIR spectroscopies. The photoelectrochemical performances of DSSCs made from these were measured and characterized, including the open-circuit voltages (VOC), short-circuit current density (JSC), fill factors (FF), and Power conversion efficiency (PCE).

2. Materials and methods

2.1. Materials

All of the chemicals and reagents utilized in this study were analytical grade and were not further purified. Glassware apparatus were used after gently washing and drying in a hot air oven at 80 °C. Iodolyte HI-30, transparent TiO₂ (Ti-Nanoxide T/SP) paste, reflective TiO₂ (Ti-Nanoxide R/SP) paste, FTO (Fluorine doped tin oxide) conducting glass were obtained from SOLARONIX Solar energy equipment supplier company, Switzerland. Acetone (CH₃COCH₃, 99.9%), Ethanol (CH₃CH₂OH, 99.9%), Methanol (CH₃OH, 99.9%), Isopropyl alcohol ((CH₃)₂CHOH, 99.5%), Dimethyl Sulphoxide (C₂C₆OS, 99%) were purchased from Pearl Chemicals, Mumbai, India. The sensitizer utilized in this investigation is an extract from the roots of the *Lawsonia inermis* plant.

Whatman filter paper, Glassware (conical flask, beakers, funnel, measuring cylinder, glass rod, Petridish), binder clips, mortar and pestle, electronic balance (AUW 320), hot air oven (Universal), muffle furnace (bio base), xenon lamp solar simulator, Keithley 2450 sourcemeter, universal LCD digital Multimeter (UNI-T UT51), UV-Vis Spectrophotometer (Jasco V-770), Fourier-transform infrared spectrophotometer (FT-IR iS550ABX thermo-scientific, Germany) and Ultrasonic bath (SJIA-950W) were the apparatuses and instruments used in the laboratory during this study.

2.2. Methods

2.2.1. Preparation of natural dye sensitizers

Natural dyes were extracted from *Lawsonia inermis* roots using a variety of solvents, including isopropyl alcohol, dimethyl Sulphoxide (DMSO), acetone, and ethanol. The dyes extracted using these solvents were produced by using the following procedure: *Lawsonia inermis* roots were washed with tap water and distilled water, peeled, and cut into smaller pieces with a plastic fruit chopper and kept in the open air for two weeks in a dark place to prevent direct sunlight. After drying for about two weeks, the samples were completely dried in an oven at 70 °C for 30 min to remove any remaining moisture content. The dried root ingredients were ground into powder using a mortar and pestle. For extraction, two grams of plant material powder were immersed separately in each 50 mL of five different and relatively nontoxic solvents (isopropyl alcohol, dimethyl sulphoxide (DMSO), acetone, and ethanol) in five 100 mL beakers for three days in the dark. After three days, the sample was filtered through filter paper. The solids were then filtered out. Filtrates were employed as a sensitizer without further purification or concentration. The pigment is then ready for soaking the electrode inside it and measuring the UV-vis absorption spectra.

2.2.2. Phytochemical screening of the plant extract

To detect the presence of phytochemicals in plant extracts, a qualitative screening was performed. Flavonoid, tannins, anthocyanin, carotenoid, and betalain pigments are the most often utilized natural dyes for DSSCs, and they are derived from various parts of plants. Standard methods were used to conduct phytochemical screening on the acetone, DMSO, ethanol and isopropanol extracts (Table 1).

2.2.3. Dimensioning of (TCO) substrate

Transparent fluorine-doped tin oxide (FTO) coated glass substrates (Solaronix, with a sheet resistance of 10-12 Ω/cm²) were employed as substrates [12]. A multimeter was used to detect the conducting side of

the glass. Alternatively, the conducting side of the glass is the side that feels foggy when lightly brushing the finger over it. To avoid contamination, the TCO glasses were handled with hand gloves rather than bare fingers. A diamond glass cutter was used to cut substrate into 2.5 cm by 2.5 cm pieces. The substrate's cell active area was adjusted to 0.3 cm by 0.4 cm (0.12 cm²).

2.2.4. Preparation of Conductive FTO Glass

The FTO conducting glass cleaning process is thought to be the most important factor influencing the final performance of the devices. Depending on the level of cleaning, a substantial effect on photovoltage behaviour can be observed experimentally [16]. As a result, FTO glass substrates were extensively cleaned before film deposition. The glass was cleaned using the following steps: first, with detergent in tap water and rinsed with distilled water; second, acetone; third, isopropanol; and, lastly, ethanol. Each solvent was used for around 25 minutes to finish the cleaning procedure in an ultrasonic bath. The conductive glass was then dried with an air gun.

2.2.5. Preparation of photoanode

Following the cleaning and drying of the FTO glasses, the photo-anode (working electrode) and the counter-electrodes were prepared as follows. TiO₂ nanoparticle pastes (Ti-Nanoxide T/SP - resulting transparent layer, colloidal anatase particles and size 15-20nm and Ti-Nanoxide R/SP - resulting reflective layer, colloidal anatase particles and size >100 nm) were coated one after another pre-cleaned FTO conducting glasses (sheet resistance 10-12Ω/cm²) by a doctor blading like technique. The doctor blading like method is the most basic and extensively used method for depositing TiO₂ paste on a substrate. It spreads TiO₂ paste over the glass with a strong squeegee or stirring rod instead of the blade [17]. These pastes were applied in the following steps:

Step 1- Coating of Ti-Nanoxide T/SP transparent paste

For the deposition of transparent active mesoporous layers, we used Ti-Nanoxide T/SP, a transparent active layer with a well-dispersed titania nanoparticle paste. The FTO glass was wrapped with adhesive tape on two parallel edges with the conductive side facing up to control the thickness of the TiO₂ layer, to keep the glass stable when applying the paste, and to provide non-coated portions for electrical contact. The paste was placed to one of the conducting glass's free edges and evenly spread using a glass rod sliding over the tape-covered edges. The T/SP, a transparent active layer, was allowed to dry at room temperature for an hour to form a levelled layer before being treated with a temperature of 1200 °C for one hour. At this temperature, we observed a colour change to a light-yellow colour.

The coated films were gradually heated in a muffle furnace at 1900 °C for 15 minutes, 2900 °C for 15 minutes, 3500 °C for 15 minutes, 4000 °C for 15 minutes, and 4500 °C for 30 minutes. Then we leave it to cool overnight by turning off the heat source until the sample achieves optimal temperature (room temperature); direct exposure to significant temperature changes could induce deformation of the titanium nanoparticle layer, that is why we used a progressive heating and cooling method. After the sintering process, the colour of the film changes to a light blue colour.

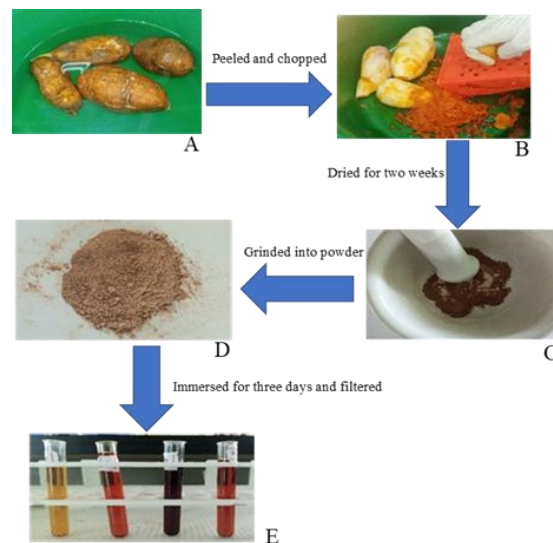


Figure 2. Extraction procedure of the natural dye (A) roots of *Lawsonia intermis*, (B) peeling and chopping, (C) crushing into powder (D) the powder after grinding, (E) dyes after soaking in isopropanol, ethanol, DMSO, and acetone solvents from left to right.

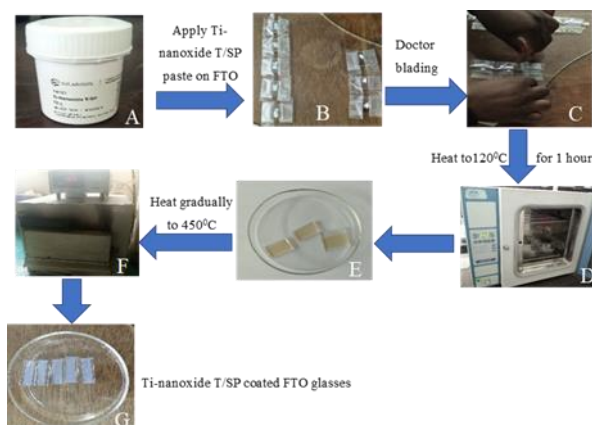


Figure 3. (A) T/SP transparent active layer, (B) Applying titanium T/SP paste on the conductive side of FTO substrate, (C) Spread the paste by a glass rod (doctor blade technique), (D) Heat the film in an oven for one hour at 1200C (E) Light yellow colour of the film (F) Sintering of the film to 4500 °C in a muffle furnace (G) The resulting film after sintering process.

Step 2- Coating of Ti-Nanoxide R/SP reflective paste

At this point, we apply Ti-Nanoxide R/SP add-on layer, big titania particle paste for reflective layer deposition, on the top of a pre-existing Ti-Nanoxide T/SP transparent active layer, and repeat the sintering process. As in the first stage, scotch tape was applied to both sides of the conductive glass. The R/SP add-on layer film was then coated on top of the T/SP transparent active layer. The T/SP is a transparent active layer coated FTO glass, which is then equally coated with the R/SP add-on layer. The Ti-Nanoxide R/SP add-on layer was allowed to cure at room temperature for one hour before being treated in an oven at 120 °C for one hour. The material was then moved to the muffle furnace and gradually heated to 450°C as the transparent layer.

Table 1. Methods of phytochemical screening.

Phytochemicals	Procedure	Indication	References
Flavonoid	1ml extract + few drop of 10% NaOH + few drops of dilute HCl (Alkaline reagent test)	Colourless	[12]
Tannins	1ml extract + 3ml distilled water + 3 drops of 10% ferric chloride solution (Braymer's test)	Blue-green colour	[13]
Anthocyanin	1ml extract + concentrated H ₂ SO ₄ (acid test)	Yellowish colour	[12]
Carotenoid	Extract + chloroform + drops of concentrated H ₂ SO ₄ (test for carotenoids)	Deep-blue coloured layers	[14]
Betalains	1ml extract + 3 drops of 2M HCl, heating for 5min at 100°C + a few drops of 2M NaOH (test for betalains)	Yellow colour	[15]

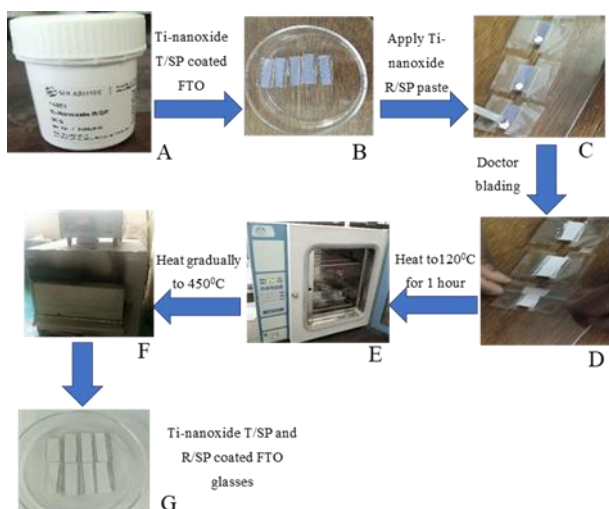


Figure 4. (A) Ti-Nanoxide R/SP reflective add-on layer (B) transparent active layer coated substrate (C) applying a reflective layer (D) spreading the reflective layer (E) Heat the layer in an oven for one hour at 1200 °C, (F) Sintering of the layer to 4500 °C in a muffle furnace (G) The resulting film after sintering.

2.2.6. Electrode sensitization

Films were warmed up to a higher temperature (800C) before being immersed in the dye solution to reduce the amount of water vapor inside the pores of the semiconductor electrode. Sensitization was performed at room temperature for 48 hours with natural dyes. During this time, the dye molecules bound to the TiO₂ and this helped in the sensitization of the semiconductor. The best way to adsorb a natural sensitizer to the oxide layer is to dip the electrode in a ready-made dye solution. Following sensitization, The TiO₂ film is taken out of the dye solution and rinsed with ethanol to remove the excess dye, but not the ethanol extracted dye-based photoanode to prevent washing out of dye molecules. Isopropanol was used to rinse ethanol extracted dye based photoanode.

2.2.7. Preparation of graphite coated counter electrode and cell assembly

The graphite covering on the counter electrode acts as a catalyst for dye reduction. To prepare the counter (positive) electrodes, the cleaned FTO substrates were coated with carbon on the conducting side using a graphite rod or soft pencil applying a light carbon film to the whole conductive side of the plate as shown in Figure 5A, then any loose graphite particles were carefully removed. This thin carbon layer catalyses the redox electrolyte regeneration reaction.

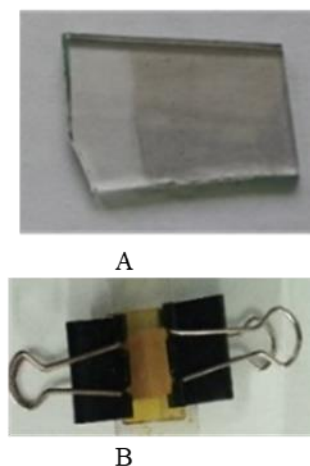


Figure 5. (A) Graphite-coated counter electrode and (B) assembled DSSC.

We withdrew the soaked photoanode from the dye solution, clamped the photoactive and counter electrodes together with the conductive side facing up, and filled the clamped cells with electrolyte drops. They should be placed so that they are slightly offset to allow connections (for the crocodile clips). We employ a commercial electrolyte based on I/I₃ in ACN (Solaronix, Iodolyte HI-30). After applying the electrolyte, as shown in Figure 5 B, the two electrodes were pressed against the electrolyte and clamped firmly in a sandwich configuration by binder clips to form a DSSC.

2.3. Spectroscopic and photoelectrochemical characterization

The dye absorption spectra were measured using a Jasco V-770 UV-Vis Spectrophotometer. The absorption is measured in ultraviolet and visible light. The band gap of dye absorbed by the TiO₂ surface is computed using the formula in equation (1). Where h denotes the Planck's constant, ν the frequency, λ the wavelength maximum absorbance of the dyes, and c the speed of light. The symbols have numerical values of $h = 6.63 \times 10^{-34}$ Js, $c = 3.0 \times 10^8$ m/s, $1\text{eV} = 1.60 \times 10^{-19}$ J, and E stands for photon energy.

$$E_{ev} = h\nu = \frac{hc}{\lambda_{max}} \quad (1)$$

FTIR spectroscopy is performed to identify the functional group present in the dyes before and after adsorption into TiO₂ nanoparticles.



Figure 6. Setup of solar simulator and I-V measurement systems.

Characterization equipment for testing the performance of solar cells with the Keithley 2450 sourcemeter and solar simulator as shown in Figure 6. Kick-start software was used to generate the I-V curves. The I-V curve was used to calculate the short circuit current I_{sc} and the open circuit voltage V_{oc} . Using the formulas in (1) and (3) the fill factor FF and η was calculated.

3. Results and discussion

3.1. UV-vis spectroscopic analysis

The performance of the dye sensitizer to absorb light and the passage of the ejected electron through the mesoporous TiO_2 layer are both essential to a DSSC's overall performance [18]. For all dyes prepared, UV-vis spectroscopy was performed using Jasco V-770 UV-Vis Spectrophotometer in the wavelength range of 200-800 nm. The UV-vis absorption spectra of the dyes extracted from the roots of Henna (*Lawsonia intermis*) plant with different solvents are shown in Figure 7. All of the dye extracts showed maximal absorption in the UV region, however a significant broad absorption in the visible region is also observed which is an important property as a sensitizer

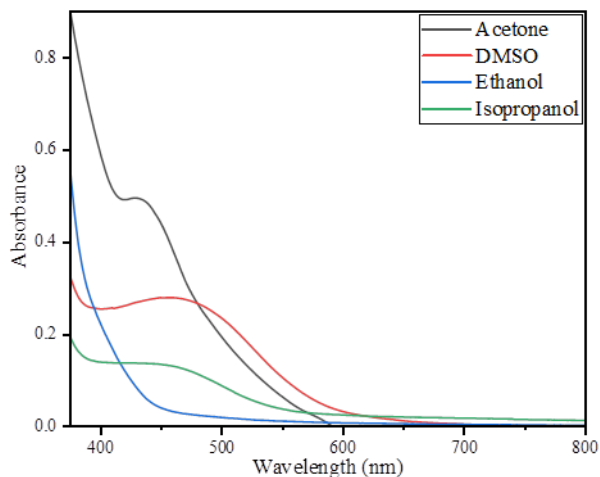


Figure 7. UV-Vis spectrum of the natural dyes extracted from roots of Henna (*Lawsonia intermis*) plant in different solvents.

The absorption peak of DMSO extract is at 450 nm, while the absorption peak of acetone extract is at 429 nm, and isopropanol at 400nm and ethanol extract have no maximum absorption in the visible region of the light spectrum as reported in literature [19], as seen in Figure 7. The above UV-Vis spectra shows the presence of much amount of

carotenoids in the roots of the *Lawsonia intermis* plant than other pigments because carotenoids absorb photons from sunlight in the visible region at wavelengths ranging from 380 nm to 550 nm [20] as shown in Figure 1. Because carotenoids have carboxyl groups as anchoring groups at the ends of their chain of molecules, they are able to attach to the interface of TiO_2 and potentially bind to it. This adsorption facilitates the transfer of the injected electron from dye to the conduction band of TiO_2 which ultimately enhances the efficiency of NDSSC. According to reports, the entire carotenoid is a poly-isoprenoid with a system of conjugated single and double bonds, which aids in the absorption of photons from sunlight in the visible range of 380 nm-550 nm. This has led to plant parts containing carotenoids have been widely investigated for use as photosensitizers in the fabrication of NDSSC. Figure 8 shows how the absorption spectra of TiO_2 films can broaden following dye adsorption at wavelengths over 400 nm. The spectrum corresponding to dye/ TiO_2 showed a non-zero absorption in the visible region of the solar spectrum. As a consequence, it was demonstrated that dye adsorption on TiO_2 surfaces can serve as a photosensitizer for DSSCs that absorb light in the visible spectrum. The absorption band of the dye has been red shifted upon chelation to TiO_2 . A non-zero absorption for dye/ TiO_2 was also observed in spectrum of visible light. Due to the wideband gap of TiO_2 (3.2 eV), bare TiO_2 do not absorb visible light, hence, no absorption band is seen in the region extending from 400 nm to 700 nm as exhibited in Figure 8.

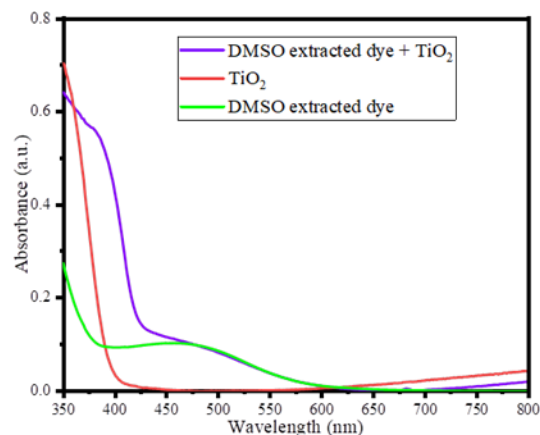


Figure 8. UV-vis absorption spectrum of TiO_2 electrode and DMSO dye before and after adsorption on the TiO_2 surface.

3.2. Optical bandgap estimation of the dyes

There is an energy differential between the conduction band and the valence band, which is known as the energy band gap and is used to analyse the performance of DSSC in relation to solar energy absorbed. The point on the absorption spectrum where the least amount of energy is needed for an electronic transition is known as the absorption edge. The energy band-gap of the solution can be found using the wavelength at the absorption edge [21]. The values of band gap of dyes extracted from roots of *Lawsonia intermis* at different solvent are given in Table 2. The optical band gap energy of this natural dye extracted this plant has been determined by using (equation 1) [22]. The lowest band gap of the dye extracted with DMSO was 2.75 eV, while root extracted with acetone and isopropanol had a band gap as high as 2.87 eV and 3.1 eV.

A dye with a low band gap allows electrons to flow quickly from the valence band to the conduction band, using less energy for the exciton formation and resulting in a higher efficiency. Therefore, DMSO extract has showed higher efficiency among extracted solvent due to low band gap.

Table 1. Absorption peaks in the visible region of all the dyes extracted and their bandgap energy.

Plant	Extracting solvent	Peak absorbance (nm)	Absorption range (nm)	Bandgap (eV)
Roots of	DMSO	450	400-600	2.75
<i>Lawsonia</i>	Acetone	429	400-500	2.87
<i>inermis</i>	Ethanol	No peak	400-450	----
	Isopropanol	400	400-500	3.1

3.3. Phytochemical Screening

For DSSC applications, dyes have frequently been employed as crude extracts (extracts without separation). The crude extracts of plants contain a variety of components that influence absorbance and, in turn, the effect of the DSSC on IPCE. In order to determine how the presence of such organic compounds was affected by the extraction solvent, a phytochemical screening was carried out. Most plant roots contain phytochemicals such flavonoids, tannins, anthocyanins, carotenes, and betalains, which were the target substances since they have important roles to play in DSSC. The phytochemical components of all plant extract samples were tested qualitatively and the result shown on Table 3.

The root of *Lawsonia inermis* plant demonstrated the presence of carotenoids in all extracting solvents, with the exception of ethanol; nevertheless, betalains and flavonoids are present in all extracting solvents, while anthocyanins were not found in any solvent extract. From the intensity of its colour, this plant root indicated the existence of more carotenoids than any other phytochemicals, because carotenoids naturally occur in red, orange, and yellow colours, and they are much more prevalent in DMSO extracts than in extracts from other solvents. This result supports higher light absorption from 380 nm to 550 nm as indicated in Figures 7; improved IPCE is expected from this extract.

Table 3. The phytochemicals present in root of *Lawsonia inermis* plant extracted with different solvents.

Phytochemicals	Extract with different solvents			
	DMSO	Ethanol	Isopropanol	Acetone
Flavonoids	+	+	+	+
Tannins	+	+	-	-
Anthocyanins	-	-	-	-
Carotenoids	++	-	+	+
Betalains	+	+	+	+

Key for results: ++ = enhanced positive result, + = positive result, - = Negative result.

Every sample of these extracts not contain anthocyanins. From the light absorption graph (Figure 7), which don't exhibit any peak or elevation in the range between 460 and 550 nm where anthocyanins absorb, serve as proof that there are no anthocyanins present, this is also confirmed by the phytochemical screening. As shown by a modest elevation, additional pigments may be responsible for the relatively high absorbance for isopropanol and DMSO extracts in this region. In general, the extraction solvents have a significant impact on the presence and amount of phytochemicals, which has an impact on both the light absorption and power conversion efficiency of the DSSCs.

3.4. Fourier Transform Infrared (FTIR) Characterization

FTIR was performed for the extracted dye with maximum power conversion efficiency (i.e., for DMSO extract), TiO₂ nanoparticle, and after adsorption of DMSO extract dye on TiO₂ nanoparticle to know the functional groups present in it. The adsorption of dye on TiO₂ nanoparticles is reaffirmed from the FTIR spectra shown in Figures 9. It was previously reported that the natural dyes extracted with functional groups such as (-COOH), (-OH), and (C=O) [23] showed higher efficiency. To ensure the presence of any of these groups in the dyes extracted, FTIR was taken in 400 cm⁻¹ – 4000 cm⁻¹ region for these samples.

The C=O stretch is responsible for the peak at 1657 cm⁻¹. O-H stretching vibration causes the strong and broad bands at 3000 cm⁻¹-3700 cm⁻¹ to exist. The C-O stretching vibrations, which stands for the esters group, are attributed to the FTIR spectra from the peaks at 1050 cm⁻¹ and 1092 cm⁻¹. The C-C stretching vibration in the aromatic group corresponds to the peaks at 1414 cm⁻¹ and 1311 cm⁻¹. The C-H bond stretching vibration is indicated by the two peaks at 2998 cm⁻¹ and 2913 cm⁻¹. It is possible that the absence of these distinctive peaks in the FTIR spectra of TiO₂ nanoparticles before they were soaked with DMSO dye was due to the highest purity of the nanoparticles in anatase crystal forms after calcination at 450 °C. Due to the improved purity of the nanoparticles in anatase crystal forms after calcination at 450 °C, these distinctive peaks in the FTIR spectra of TiO₂ nanoparticles before DMSO dye treatment may not have been present. The Ti-O stretching bands, which were attributed to the TiO₂ nanoparticles having an anatase structure, were responsible for the remaining peak between 500 cm⁻¹ and 400 cm⁻¹ found for bare TiO₂ nanoparticles.

The existence of the carboxylic acid group in the plant extract is demonstrated by the FTIR analysis of the DMSO dye (-COOH) as shown in Figure 9, can established an electronic coupling with the conduction band of TiO₂ and help to anchor the dye molecules and bring towards an effective electron injection to the conduction band of TiO₂.

3.5. The effect of solvent extraction on DSSC efficiency

By changing the solvent, the effect of extracting solvent on DSSC performance was investigated. The sensitizing performance of natural pigments varies depending on the source from which the natural pigments are taken. Extraction solvents of these natural dyes must be carefully selected in order to obtain high extraction efficiency. It has

been reported that the solubility of different dyes varies depending on the polarity of the extraction solvent, influencing the solubility and anchoring behaviour of sensitizing dyes onto TiO_2 , hence affecting cell conversion efficiency. Many organic solvents are often used to extract natural pigments, and the polarity of the solvent can influence the absorption spectra of dyes, the amount of dyes extracted, and the diffusion of dyes onto the surface of TiO_2 , therefore careful solvent selection is critical.

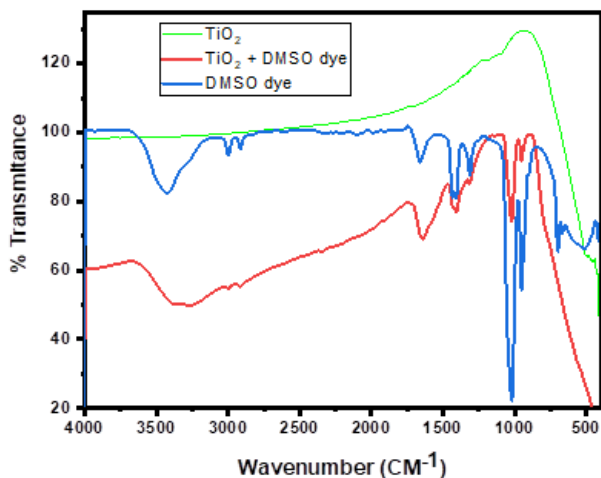


Figure 9. FTIR analysis for DMSO dye, TiO_2 nanoparticle and DMSO dye adsorbed on TiO_2 nanoparticles.

In this study, as extracting solvents, four distinct solvents were used: DMSO, isopropanol, acetone, and ethanol. Figure 10 depicts typical current density-voltage (J-V) curves of DSSCs made using dyes extracted from the roots of *Lawsonia inermis* plant using DMSO, isopropanol, acetone, and ethanol as extracting solvents. Table 4 shows the PEC parameters that were collected.

As shown in J-V curve, the efficiency of the DSSCs was found to increase immensely when DMSO was used for extracting pigments. This might be due to the fact that our extracted pigments in DMSO solvent have wide and intense absorbance in visible region of solar spectrum, and pigments in the plant are more soluble in DMSO than other solvents, as a result; the aggregation of dye molecules decreases as expected. Better dispersion of dye molecules on the oxide surface could exactly improve the efficiency of the system.

3.6. J-V Characteristic Measurement of DSSCs

Artificial sun/solar simulator provide illumination approximating natural sunlight. The purpose of solar simulators is to provide a controllable indoor test facility under laboratory conditions and they are fundamental devices for characterization of photonic properties. Solar simulators have a light source that is designed to offer a similar intensity and spectral composition to that of natural light.

The current-voltage characteristics of all dye sensitizers that were used in the research were measured using artificial light source which can simulate the sun's illumination. In this research we have used xenon lamp solar simulator with the standard AM1.5G to simulate the sun at

$100\text{mW}/\text{cm}^2$ (full day light). The most important factor in any solar cell characterization is the intensity of the light. So, it is necessary to examine cells under a consistent illumination setup for measurements from various research groups to be fairly compared. The National Renewable Energy Laboratory (NREL) of the United States established the first PV characterisation criteria in the 1980s. The Standard Reporting Conditions mandate that cell performance be measured using an AM 1.5 spectrum reference or $1\text{kW}/\text{m}^2$ of light irradiance. A reference solar cell is often used to calibrate the irradiance in the characterisation. The typical current density-voltage (J-V) curves of the DSSC fabricated with the dyes extracted from the roots of *Lawsonia inermis* plant using isopropanol, ethanol, acetone and DMSO as extracting solvent are shown in Figure 10. The PEC parameters obtained are given in Table 4.

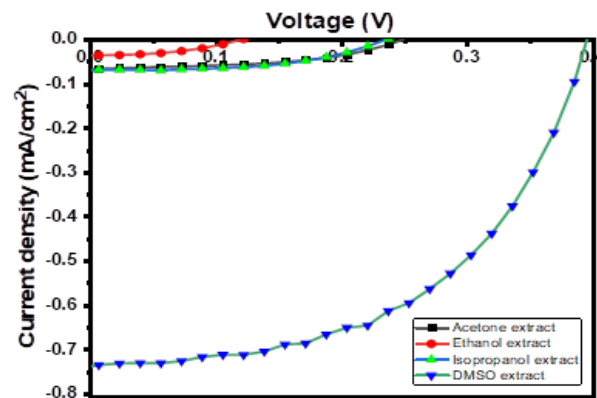


Figure 10. Current density-voltage curves of DSSCs sensitized with dye extracted from *Lawsonia inermis* roots in ethanol, acetone, isopropanol, and DMSO solvents.

The results of each parameter that have been obtained was 0.188 mA cm^{-2} of short circuit current density, 0.388 V of open circuit voltage, 0.2209 of power conversion efficiency for DMSO extract, 0.066 mA cm^{-2} of short circuit current density, 0.25 V of open circuit voltage, 0.085 of power conversion efficiency for acetone extract, 0.07 mA cm^{-2} of short circuit current density, 0.235 V of open circuit voltage and 0.082 of power conversion efficiency for isopropanol extract and 0.0354 mA cm^{-2} of short circuit current density, 0.121 V of open circuit voltage and 0.019 of power conversion efficiency for ethanol extract.

The greater J_{sc} , V_{oc} , and η values were obtained for the DSSC sensitized from the DMSO extract of *Lawsonia inermis* roots, as can be seen from the figure above, while the lowest J_{sc} , V_{oc} , and values were obtained for the ethanol extract of dye. From the phytochemical analysis DMSO extract is found to be rich in carotenoids, flavonoids, betalains and tannins. Such a composition may contribute for the greater power conversion efficiency. This is a result of good interaction of TiO_2 with plant pigments that was extracted from *Lawsonia inermis* roots using DMSO solvent, which led to good charge transfer and enhanced pigment solubility in DMSO solvent. By displacing an OH^- counter ion from the Ti (IV) site and combining it with a proton that is provided by the carotenoids, this carotene quickly adsorbed to the surface of TiO_2 .

Power conversion efficiency of DSSC obtained from this work were compared with other natural dyes extracted from root so far by other groups as showed in Table 4. DSSC fabricated from dye of *Lawsonia inermis* root extract by using DMSO as a solvent shows the highest power conversion efficiency than using acetone, isopropanol or ethanol. This might owe to the fact that pigments (mainly carotenoid) in this plant are more soluble in DMSO, and hence, the aggregation of dye molecules is less as expected. Therefore, the extracting solvent has an effect on the efficiency of DSSCs as shown in Table 4.

Plant	Solvents	J_{sc} (mA cm ⁻²)	V_{oc} (mV)	FF (%)	η (%)	Ref.
Roots of <i>Lawsonia inermis</i>	DMSO	0.734	390	51.35	0.15	This work
	Acetone	0.066	250	46.487	0.085	
	Isopropanol	0.07	235	45.028	0.082	
	Ethanol	0.0354	121	39.768	0.019	
Carrots (<i>Daucus carota</i>)	Acetone	0.136	385	47.6	0.037	[24]
Beetroot (<i>Beta vulgaris</i>)	Aqueous extract	1.295	380	32	0.15	[25]
Ginger (<i>Zingiber officinale</i>)	Acetone	0.16	111	72	2.02	[26]

3.6.1. Effect of various light intensities on the performance of DSSC

The photovoltaic performance of dye-sensitized solar cells (DSSCs) installed in a particular area can vary significantly as a result of a number of natural factors, including seasonal changes, sunlight irradiation, and locally windy and cloudy conditions [27]. DSSCs have been studied extensively in the past under the typical 1-Sun situation (i.e., 100 mW cm²) for their characterisation. Due to the absence of pertinent information about DSSCs tested at varied light intensities, the fundamental understanding of the functioning and practical uses of DSSCs may thus be limited. In order to examine the effect of operating intensity of light on the photovoltaic performance of the DMSO extract based DSSC, we varied the operating light of the DSSCs by placing neutral density (ND) filters and a condenser lens in the illumination path.

The recombination of TiO₂ conduction band electrons via surface-state-mediated electron transfer into the electrolyte can be used to explain why the PCE decreases at low incident light intensities. However, at high light intensities, the PCE of DSSCs increased because there were more photogenerated electrons present. This led to a rise in the amount of electrons injected into the TiO₂ nanoparticles, while at the same time, charge recombination's capability to lose electrons was mitigated [28]. The J_{sc} values show a considerable rise with an increase in light intensity, as seen in Figure 11 and Table 5. V_{oc} values for various operating light intensities, however, don't seem to alter all that much. These results in

increase the power conversion efficiency of the solar cell. This is because increasing light concentration results in an increase in power intake.

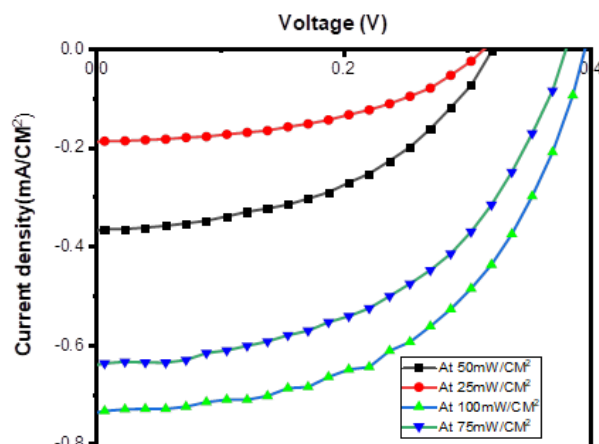


Figure 11. Current density-voltage curve for different light intensities illuminated on DMSO extracted DSSCs.

Table 5. Electrical properties of a DMSO extract based DSSCs under different light intensities.

Light intensity	J_{sc} (mAcm ⁻²)	V_{oc} (mV)	FF (%)	η (%)
25 mW/cm ²	0.187	310	35.65	0.021
50 mW/cm ²	0.366	320	38.376	0.045
75m W/cm ²	0.638	380	40.446	0.098
100 mW/cm ²	0.734	390	51.35	0.15

4. Conclusions

Natural dyes extracted from *Lawsonia inermis* roots were used as sensitizers in DSSCs. *Lawsonia inermis* root investigated in this research have never been studied for the purpose of fabrication of dye-sensitized solar cells. From the phytochemical analysis and optical characteristics carotenoids are typically found in dyes produced from this plant material. Among the solvents DMSO extract dye sensitized solar cell showed the best photoelectrochemical performance, with a V_{oc} of 0.39 V, a J_{sc} of 0.734 mA/cm², and a power conversion efficiency of 0.15%. The extraction solvents have a significant impact on the presence and amount of phytochemicals, which has an impact on both the light absorption, optical energy gap and power conversion efficiency of the DSSCs. The power conversion efficiency of the DSSCs is also affected by the amount intensity

Declaration of competing interest

The authors declare that they have no competing interests.

Acknowledgments

The authors gratefully acknowledge Addis Ababa Science and Technology (AASTU).

References:

1. A. Mohammad Bagher, Types of Solar Cells and Application, Am. J. Opt. Photonics 3 (2015) 94.

2. V. Muteri, M. Cellura, D. Curto, V. Franzitta, S. Longo, M. Mistretta, and M. L. Parisi, Review on Life Cycle Assessment of Solar Photovoltaic Panels, *Energies* 13 (2020) 252.
3. P. Roy, N. Kumar Sinha, S. Tiwari, and A. Khare, A review on perovskite solar cells: Evolution of architecture, fabrication techniques, commercialization issues and status, *Sol. Energy* 198 (2020) 665.
4. H. Michaels, M. Rinderle, R. Freitag, I. Benesperi, T. Edvinsson, R. Socher, A. Gagliardi, and M. Freitag, Dye-sensitized solar cells under ambient light powering machine learning: towards autonomous smart sensors for the internet of things, *Chem. Sci.* 11 (2020) 2895.
5. M. Green, K. Emery, Y. Hishikawa, W. Warta, E. Dunlop, D. Barkhouse, O. Gunawan, T. Gokmen, T. Todorov, and D. Mitzi, Prog. Solar cell efficiency tables (version 40), *Photovoltaics Res. Appl.* 20 (2012) 1114.
6. M. Grätzel, Solar Energy Conversion by Dye-Sensitized Photovoltaic Cells, *Inorg. Chem.* 44 (2005) 6841.
7. B. O'Regan and M. Gratzel, A Low-Cost, High-Efficiency Solar Cell Based on Dye-Sensitized Colloidal TiO₂ Films, *Nature* 354 (1991)737.
8. N. Puspitasari, S. S. Nurul Amalia, G. Yudoyono, and Endarko, Effect of Mixing Dyes and Solvent in Electrolyte Toward Characterization of Dye Sensitized Solar Cell Using Natural Dyes as the Sensitizer, *IOP Conf. Ser. Mater. Sci. Eng.* 214 (2017).
9. R. Adel, T. Abdallah, Y. M. Moustafa, A. M. Al-Sabagh, and H. Talaat, Effect of polymer electrolyte on the performance of natural dye sensitized solar cells, *Superlattices Microstruct.* 86 (2015) 62.
10. S. Tadesse, A. Abebe, Y. Chebude, I. Villar Garcia, and T. Yohannes, Natural dye-sensitized solar cells using pigments extracted from *Syzygium guineense*, *J. Photonics Energy* 2 (2012) 1.
11. G. Yirga, S. Tadesse, and T. Yohannes, Photoelectrochemical Cell Based on Natural Pigments and ZnO Nanoparticles, *J. Energy Nat. Resour.* 5 (2016) 1.
12. J. B. Harborne, *Phytochemical Methods: A Guide to Modern Techniques of Plant Analysis*, Second edi (CHAPMAN AND HALL, New York, 1973).
13. P. O. Ukoha, E. A. C. Cernaluk, O. L. Nnamdi, and E. P. Madus, Tannins and other phytochemical of the *Samanea saman* pods and their antimicrobial activities, *African J. Pure Appl. Chem.* 5 (2011) 237.
14. B. C. Mphande and A. Pogrebnoi, Impact of extraction methods upon light absorbance of natural organic dyes for dye sensitized solar cells application Impact of Extraction Methods upon Light Absorbance of Natural Organic Dyes for Dye Sensitized Solar Cells Application, *J. Energy Nat. Resour.* 3 (2014)38.
15. J. Swarna, T. S. Lokeswari, M. Smita, and R. Ravindhran, Characterisation and determination of in vitro antioxidant potential of betalains from *Talinum triangulare* (Jacq.) Willd, *Food Chem.* 141 (2013) 4382.
16. P. J. Cameron, L. M. Peter, and S. Hore, How Important is the Back Reaction of Electrons via the Substrate in Dye-Sensitized Nanocrystalline Solar Cells, *J. Phys. Chem. B* 109 (2005) 930.
17. O. Adedokun, M. K. Awodele, Y. K. Sanusi and A.O Awodugba, Natural dye extracts from fruit peels as sensitizer in ZnO based dye-sensitized solar cells, *IOP Conf. Series: Earth and Environmental Science* 173 (2018) 012040.
18. W. Ghann, H. Kang, T. Sheikh, S. Yadav, T. Chavez-Gil, F. Nesbitt, and J. Uddin, Fabrication, optimization and characterization of natural dye sensitized solar cell, *Sci. Rep.* 7 (2017) 41470.
19. S. Sowmya, Pooja Prakash, N. Ruba, B. Janarthanan, A. Nagamani Prabu, and J. Chandrasekaran, A study on the fabrication and characterization of dye-sensitized solar cells with *Amaranthus red* and *Lawsonia inermis* as sensitizers with maximum absorption of visible light, *J. Mater. Sci. Mater. Electron.* 31 (2020) 6027.
20. A. Singh and T. Mukherjee, Application of carotenoids in sustainable energy and green electronics, *Mater. Adv.* 3 (2022) 1341.
21. S. Myat and S. N. Khine, Optical properties of dye solutions for dye-sensitized solar cell, *Int. J. Sci. Res. Publ.* 8 (2018) 32.
22. A. Slav, Dig. Optical Characterization of TiO₂-Ge Nanocomposite Films obtained by reactive magnetron sputtering, *J. Nanomater. Biostructures*, 6 (2011) 915.
23. S. Sowmya, N. Ruba, K. Inbarajan, P. Prakash, and B. Janarthanan, A novel idea of using dyes extracted from the leaves of *prosopis juliflora* in dye sensitized solar cells, *Opt. Quantum Electron.* 120 (2021) 111429.
24. A. S. H Hardani, LM Angraeni, C Cari, Improved Performance of Dye-Sensitized Solar Cells With TiO₂,” *J. Fis. Flux*, vol. 16, (2019) 61.
25. M. A. Almutairi, W. A. Farooq, and M. S. AlSalhi, Photovoltaic and impedance properties of dye-sensitized solar cell based on nature dye from beetroot, *Curr. Appl. Phys.* 40 (2022)119.
26. T. T. Win, Y. M. Maung, K. K. K. Soe, Comparison on Photo-Electro Chemical Properties of ZnO Electrode with Different Natural Dyes, *PCO Proceeding 2008* (2013) 181
27. B. Tripathi, P. Yadav, and M. Kumar, Charge transfer and recombination kinetics in dye-sensitized solar cell using static and dynamic electrical characterization techniques, *Sol. Energy* 108 (2014) 107.
28. J. H. Kim, K. J. Moon, J. M. Kim, D. Lee, and S. H. Kim, Effects of various light-intensity and temperature environments on the photovoltaic performance of dye-sensitized solar cells, *Sol. Energy* 113 (2015) 251.